ISBN: 978-3-95450-220-2 ISSN: 2673-5474 doi: 10.18429/JACoW-FEL2022-TUBO3

COMPARISON OF TRANSVERSE COHERENCE PROPERTIES IN SEEDED AND UNSEEDED FEL

M. Pop*, F. Curbis, S. Werin, Physics department, Lund University, Lund, Sweden
A. Simoncig, C. Spezzani, D. Garzella, E. Allaria , G. De Ninno, G. Perosa,
G. Penco, L. Foglia , L. Giannessi, M. Zangrando, M. Trovo,
M. Manfredda , N. Mahne, N. Mirian, P. R. Ribic,
S. Di Mitri , S. Spampinati, Elettra-Sincrotrone, Trieste, Italy
G. Geloni, European XFEL, Hamburg, Germany
N. Mirian, Deutsches Elektronen-Synchrotron (DESY), Hamburg, Germany

Abstract

The transverse coherence of the source is an important property for FEL experiments. Theory and simulations indicated different features for seeded and unseeded FELs but so far no direct comparison has been pursued experimentally on the same facility. At FERMI FEL one has the unique possibility to test both SASE and seeded configurations under the same operating conditions. In this contribution we present the experimental results of the characterization of transverse coherence with special attention to the evolution of this fundamental property.

INTRODUCTION

Novel investigation techniques such as diffractive imaging [1] and X-ray holography [2] require high levels of transverse coherence from the free electron laser (FEL) source. An X-ray FEL is usually driven by a high current, low emittence and low energy spread electron beam. To achieve ultra relativistic velocities and high currents, the electron beam is accelerated by a linear accelerator and compressed by dispersive sections called bunch compressors. After acceleration the beam is then fed through and undulator line called radiator where the interaction between the electrons and the electromagnetic field, which they themselves produce, exponentially amplifies the latter. The resulting FEL radiation is highly brilliant and highly coherent.

Taking advantage of the capabilities of FERMI FEL-2, we were able to study two distinct modes of operating an FEL: self amplified spontaneous emission (SASE) and seeded. The first option is able to produce gigawatts of power by directly sending the electrons through the radiator, without any prior phase space shaping [3–6]. The longitudinal coherence of SASE radiation can be improved if the FEL is seeded [7–9]. The most common seeding scheme, in the XUV range, is the high gain harmonic generation or HGHG. First, an external laser co-propagating with the electron beam inside an undulator, called modulator, imprints an energy modulation onto the electron beam. Then the energy modulation is transformed into density modulation in a dispersive section. Such density modulation exhibits bunching not only at the fundamental harmonic but, with diminishing intensities, also at higher harmonics. By this mechanism HGHG FELs can produce longitudinally coherent radiation at harmonics of the wavelength an external, optical laser.

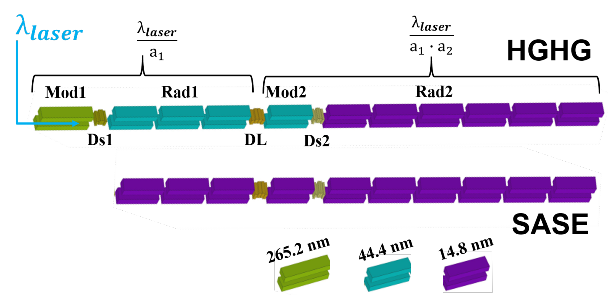

Figure 1: Schematic layout of FERMI FEL-2 operated in cascaded HGHG (top) and SASE (bottom) modes. The undulators are color-coded to the resonant wavelength they were set during the experiment.

Previous work showed that both SASE [10, 11] and seeded [12] FELs reach high degrees of transverse coherence. Furthermore, semi-analytical and simulation studies indicated that in a SASE FEL the transverse coherence is built up during the amplification process, reaching a maximum before intensity saturation. Aiming at qualitatively comparing the evolution of transverse coherence, this contribution presents the first experimental confirmation of the early saturation of this property in SASE FELs. A more in-depth description and analysis is presented in the original paper describing this experiment [13].

EXPERIMENTAL SETUP

The aim of our experiment was to estimate the transverse coherence properties of the FERMI FEL-2, operated in cascaded HGHG (seeded) and SASE modes. By progressively tuning out radiators, it is possible to obtain a transverse coherence gain curve which can be used to investigate how coherence is built up in the two types of FEL.

FERMI FEL-2 is usually run in fresh-bunch cascaded HGHG mode [14], which can produce longitudinally coherent pulses down to a few nanometers. However, for this

* corresponding author: mihai.pop@maxiv.lu.se

ISBN: 978-3-95450-220-2
ISSN: 2673-5474
doi: 10.18429/JACoW-FEL2022-TUBO3

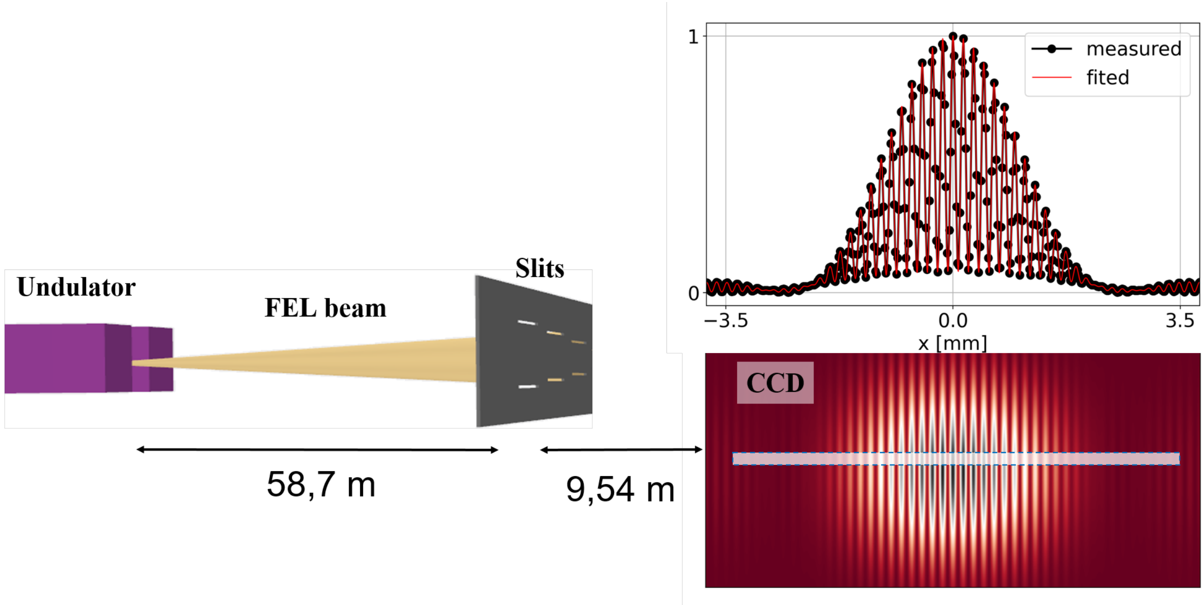

Figure 2: Layout of the measurement setup. The FEL radiation propagates 58.7 m from the end of the last undulator to the slits. The diffracted light travels 9.54 m from the slits to a CCD. The 1D interference pattern(top right) is obtained by averaging along the vertical direction of the area highlighted in white on the CCD.

experiment we chose as final radiation wavelength 14.8 nm to be able to obtain significant radiation amplification for the SASE mode of operation. As show in Fig. 1, the external laser wavelength was 266.4 nm and in the first stage the radiator was set to the 6^{th} harmonic, 44.4 nm. The second stage was made resonant to the third harmonic of the second stage, i.e., 14.8 nm. In SASE operation all undulators, with the exception of the first modulator which was fully opened, were set resonant to the final 14.8 nm wavelength.

The figure of merit we used to characterize the transverse coherence was the total degree of transverse coherence ζ [15]. In the Gauss-Schell model [11] the procedure for obtaining ζ involves determining the transverse coherence length l_c and the radiation transverse size σ. The transverse coherence length is deduced by fitting the decay of the degree of coherence $\boldsymbol{g}$ as a Gaussian. The degree of coherence is obtained by fitting the intensity of the interference pattern form a *Young double-slit* experiment to a theoretical function $I_{fit}(w, d, z, \boldsymbol{g}, ..)$ that takes into account the width w and separation d of the slits, the propagation distance from the slits to the screen z and the degree of coherence $\boldsymbol{g}$ among other things. The special fitting function used in our experiment is detailed in the appendix of the original paper [13].

The layout of the experimental setup for measuring transverse coherence is presented in Fig. 2. The diffraction pattern is recorded on a CCD camera capable of detecting single shot images. For this experiment we only investigated the horizontal direction (OX) but we expect the vertical direction to yield similar results.

RESULTS

As mentioned in the previous section, by performing the Young double-slit experiment at various slit separations one can obtain the transverse coherence length. In Fig. 3 we plot the decay of the degree of coherence $\boldsymbol{g}$ as the slit separation increases. The fitted coherence lengths are $l_{c_x}^{SASE} = 1.88 \pm 0.2$ mm and $l_{c_x}^{HGHG} = 2.2 \pm 0.1$ mm for SASE and HGHG modes of operation respectively.

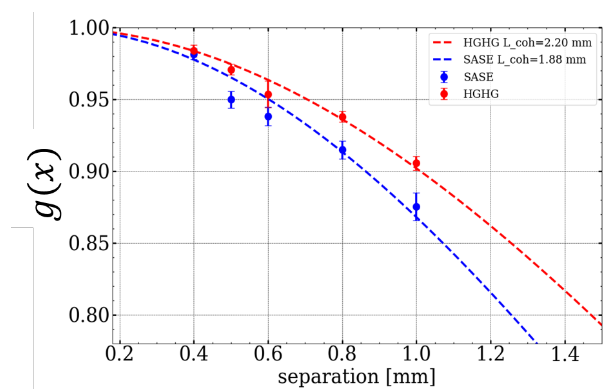

Figure 3: Measured (dots with error bars) an fitted (dashed lines) for HGHG (red) and SASE (blue) modes of operation.

The transverse coherence sizes, of the two modes were measured to be $\sigma_x^{SASE} = 1.25 \pm 0.05$ mm and $\sigma_x^{HGHG} = 1.38 \pm 0.1$ mm. These measurements, in conjunction with the transverse coherence length give the following values for the total degree of transverse coherence $\zeta_x^{SASE} = 0.6 \pm 0.03$ and $\zeta_x^{HGHG} = 0.62 \pm 0.02$.

By opening the gap of more and more undulators, we were able to obtain snapshots of the FEL radiation at different

ISBN: 978-3-95450-220-2 ISSN: 2673-5474 doi: 10.18429/JACoW-FEL2022-TUBO3

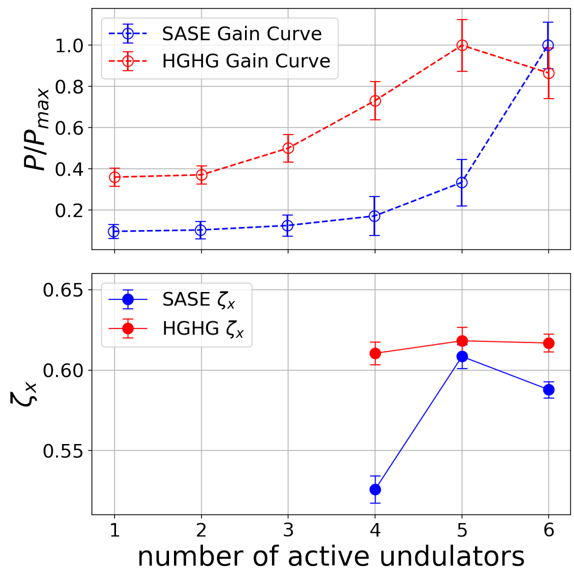

Figure 4: Intensity gain curve (top) and total degree of coherence evolution (bottom) for HGHG (red) and SASE (blue) modes of operation.

stages in the the gain process, both in terms of radiation intensity but also in terms of transverse coherence. In Fig. 4 we plot the evolution of radiation intensity (top) and transverse coherence (bottom) as a function of number of active undulators for SASE and seeded modes of operation using the transverse coherence measurement procedure described in the previous section. As stated in [13] even though the radiation intensity did not reach saturation in the available undulator length, we did manage to achieve saturation of transverse coherence.

The evolution of transverse coherence, Fig. 4 (bottom), suggests qualitatively different mechanisms for building up this property in the two modes of operation (SASE and HGHG). In the seeded case, we observe an almost constant value for transverse coherence along the gain curve, while for SASE there is a visible evolution, indicating that transverse coherence is built up similarly to longitudinal coherence. The HGHG trend suggests that seeded modes of operation "inherit" the transverse coherence from the seed laser.

The different buildup processes of seeded and SASE FEL's transverse coherence observed in the gain based data is confirmed by a complementary measurement in which the energy spread of the electron beam is varied. By using a laser heater system [16], one can induce extra, uncorrelated, energy spread into the electron beam. This has the effect of changing the gain length of the FEL. We can thus change the position in the gain curve at which we measure the transverse coherence by modifying the energy spread. In Fig. 5 we can see that the change in energy spread has a similar effect on the intensity (magenta trace) on the SASE (top) and HGHG (bottom) modes of operation. However, looking at the scaled transverse coherence we find considerably different trends between SASE and HGHG. While for HGHG it maintains at an almost constant level, for SASE the transverse coherence seems to be highly dependent on the position in the gain curve. These measurements agree qualitatively with the measurements based on tuning out undulators and strengthen the interpretation that transverse coherence develops by fundamentally different mechanisms in SASE and seeded FEL.

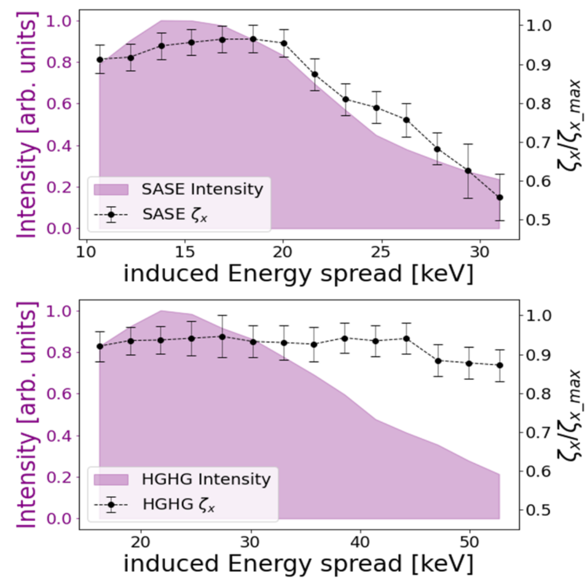

Figure 5: Intensity variation (magenta) and scaled total degree of coherence (black) with induced electron energy spread, for SASE (top) and HGHG (bottom) modes of operation.

CONCLUSIONS

At FERMI FEL-2 we were able to compare, for the first time, the HGHG and SASE modes of operation in terms of transverse coherence. In our experimental setup SASE and HGHG FEL reached similar maximum values of transverse coherence. Furthermore our data shows that the way in which the two modes of operation develop transverse coherence is fundamentally different. While in the SASE process transverse coherence is built up and reaches a maximum earlier than power saturation, in HGHG the FEL starts of with a high degree of transverse coherence and maintains it all through the amplification process.

ACKNOWLEDGEMENTS

We would like to thank the entire team of FERMI FEL for their support during and after the experiment.

REFERENCES

[1] H. N. Chapman *et al.*, "Femtosecond diffractive imaging with a soft-X-ray free-electron laser," *Nat. Phys.*, vol. 2, no. 12, pp. 839–843, 2006. doi:10.1038/nphys461

ISBN: 978-3-95450-220-2 ISSN: 2673-5474 doi: 10.18429/JACoW-FEL2022-TUBO3

[2] C. J. Jacobsen, "X-ray microscopy using FELs: possibilities and challenges," in *Proc. SPIE 3925*, International Society for Optics and Photonics, vol. 3925, 2000, pp. 16–25. doi:10.1117/12.384260

[3] R. Bonifacio, C. Pellegrini, and L. Narducci, "Collective instabilities and high-gain regime in a free electron laser," 6, vol. 50, 1984, pp. 373–378. doi:10.1016/0030-4018(84)90105-6

[4] E. Saldin, E. V. Schneidmiller, and M. V. Yurkov, *The physics of free electron lasers*. Springer Science & Business Media, 1999.

[5] L. H. Yu, "Generation of intense uv radiation by subharmonically seeded single-pass free-electron lasers," *Phys. Rev. A*, vol. 44, pp. 5178–5193, 1991. doi:10.1103/PhysRevA.44.5178

[6] P. Emma *et al.*, "First lasing and operation of an ångstrom-wavelength free-electron laser," English (US), *Nat. Photonics*, vol. 4, no. 9, pp. 641–647, 2010. doi:10.1038/nphoton.2010.176

[7] L.-H. Yu *et al.*, "High-Gain Harmonic-Generation Free-Electron Laser," *Science*, vol. 289, no. 5481, pp. 932–934, 2000. doi:10.1126/science.289.5481.932

[8] E. Allaria *et al.*, "Highly coherent and stable pulses from the FERMI seeded free-electron laser in the extreme ultraviolet," *Nature Photonics*, vol. 6, no. 10, pp. 699–704, 2012. doi:10.1038/nphoton.2012.233

[9] P. R. Ribič *et al.*, "Coherent soft X-ray pulses from an echo-enabled harmonic generation free-electron laser," *Nat. Photonics*, vol. 13, no. 8, pp. 555–561, 2019. doi:10.1038/s41566-019-0427-1

[10] R. Ischebeck *et al.*, "Study of the transverse coherence at the ttf free electron laser," *Nucl. Instrum. Methods Phys. Res., Sect. A*, vol. 507, no. 1, pp. 175–180, 2003, Proceedings of the 24th International Free Electron Laser Conference and the 9th Users Workshop. doi:10.1016/S0168-9002(03)00866-0

[11] I. A. Vartanyants and A. Singer, "Coherence properties of hard x-ray synchrotron sources and x-ray free-electron lasers," *New J. Phys.*, vol. 12, no. 3, p. 035 004, 2010. doi:10.1088/1367-2630/12/3/035004

[12] O. Y. Gorobtsov *et al.*, "Seeded X-ray free-electron laser generating radiation with laser statistical properties," *Nat. Commun.*, vol. 9, no. 1, p. 4498, 2018. doi:10.1038/s41467-018-06743-8

[13] M. Pop *et al.*, "Single-shot transverse coherence in seeded and unseeded free-electron lasers: A comparison," *Phys. Rev. Accel. Beams*, vol. 25, p. 040 701, 4 2022. doi:10.1103/PhysRevAccelBeams.25.040701

[14] E. Allaria *et al.*, "Two-stage seeded soft-X-ray free-electron laser," *Nat. Photonics*, vol. 7, no. 11, pp. 913–918, 2013. doi:10.1038/nphoton.2013.277

[15] J. W. Goodman, *Statistical optics*. John Wiley & Sons, 2015.

[16] S. Spampinati *et al.*, "Laser heater commissioning at an externally seeded free-electron laser," *Phys. Rev. ST Accel. Beams*, vol. 17, p. 120 705, 2014. doi:10.1103/PhysRevSTAB.17.120705